DEGREE PROJECT IN TECHNOLOGY,
FIRST CYCLE, 15 CREDITS
STOCKHOLM, SWEDEN 2021

Electric Self Propelled Shoe

A shoe mountable last mile personal transportation vehicle

VIKTOR KÅREFJÄRD

DAVID STRIDFELDT

KTH ROYAL INSTITUTE OF TECHNOLOGY
SCHOOL OF INDUSTRIAL ENGINEERING AND MANAGEMENT

Electric Self Propelled Shoe

A shoe mountable last mile personal transportation vehicle

VIKTOR KÅREFJÄRD
DAVID STRIDFELDT

Bachelor's Thesis at ITM
Supervisor: Nihad Subasic
Examiner: Nihad Subasic

TRITA-ITM-EX 2021:27

Abstract

The purpose of this work was to investigate how a last-mile-transport vehicle can be constructed around a shoe. The prototype, which is controlled without a handheld controller, was designed to propel an adult forward with the use of an electric driveline. The user can easily stop driving, and instead walk short distances without removing the prototype

Research questions have been answered regarding how the battery and motor can be configured to reach a top speed of 15 km/h and a range of 3 km. In addition, answers were given as to how a user should control the vehicle's speed in a safe and simple way, without the use of a handheld remote controller.

The results show that the prototype reaches the specified top speed, and that the specified range is reached and exceeded. The user controls the motor power by moving their weight from the left to the right foot. The applied weight is measured by load cells under the heel, and after calibration, this user input method can be seen as satisfactory. The electric driveline, which is mounted under the shoe, allows the user to walk short distances without removing the prototype.

Future work may add safety equipment such as lamps and a bell to make the product legal for use in public areas. In addition, a left shoe needs to be developed further, due to how the concept is dependent on it to function optimally.

Keywords: Mechatronics, last mile transport, brushless DC motor, load cell, personal transport.

Referat

Elektriskt motordriven sko

Det här arbetet hade till avsikt att undersöka hur ett sista-sträckan-fordon kan konstrueras kring en sko. Prototypen, vilken styrs utan en handkontroller, utformades för att förflytta en vuxen person med hjälp av en elektrisk drivlina. Användaren kan enkelt sluta åka, och istället gå kortare sträckor utan att ta av sig prototypen.

Forskningsfrågor har besvarats angående hur batteri och motor kan konfigureras för att uppnå topphastigheten 15 km/h och färdsträckan 3 km. Dessutom besvarades hur en användare ska kontrollera fordonets hastighet på ett säkert och enkelt sätt, utan användning av en handkontroll.

Resultaten visar att prototypen uppnår topphastigheten, och att den angivna räckvidden uppnås och överskrids. Användaren styr motoreffekten genom att förflytta sin vikt från vänster till höger fot. Den applicerade vikten mäts av lastceller under hälen, och efter kalibrering kan denna användar-inmatningsmetod ses som tillfredsställande. Den elektriska drivlinan, som monteras under skon, tillåter att användaren går kortare sträckor utan att ta av sig prototypen.

Framtida arbete kan tillägga säkerhetsutrustning, som lampor och ringklocka för att göra produkten laglig för användning på allmän plats. Dessutom behöver en vänstersko utvecklas mer, på grund av hur konceptet är beroende av denna för att fungera optimalt.

Nyckelord: Mekatronik, Sista sträckan transport, Borstlös DC motor, lastceller, personlig transport.

Contents

List of Figures

List of Tables

List of Abbreviations

3D Three Dimensional. 17

BEC Battery Eliminator Circuit. 13

BLDC Brushless Direct Current. 4, 5, 12

DC Direct Current. 4

ESC Electric Speed Controller. 5, 15, 16

I/O Input/Output. 7

Li-ion Lithium-ion. 3

LiPo Lithium-ion Polymer. 3, 4, 12, 17

PB Lead Acid. 3

PLA Polylactic acid. 17

PPM Pulse-position Modulation. 8, 16

PWM Pulse-width Modulation. 8

Chapter 1

Introduction

This chapter includes the lead-in information about the thesis, for instance the reasoning behind the project, its intentions, and some limitations.

1.1 Background

Recent developments in battery technology and microcomputers have sent rise to a number of new and exciting small personal transportation vehicles. Electric skateboards and scooters, for example, are growing in numbers [1].

When not in use, these products can have the downside of being experienced as heavy and cumbersome to carry. Furthermore, if parked they run the risk of being stolen.

Therefore, the question arises if similar technology can be incorporated into a smaller, more portable product.

1.2 Purpose

The purpose of this thesis is to investigate if an electric drivetrain can be mounted to a shoe, whilst keeping the ability to walk short distances. The shoe should have the ability to propel an adult forward in a safe and controlled manner according to commands given by the user. The thesis seeks to answer the following questions:

1. How can a battery and motor be configured to have a range of 3 km?
2. How can a battery and motor be configured to have a top speed of 15 km/h?
3. How can a suitable driveline be assembled onto a regular shoe?
4. How can the motor be controlled without using a handheld remote controller?

1.3 Scope

This thesis was limited in some ways to make the project reasonable. The size of the shoes was naturally an important factor, since larger shoes can fit larger components. In order to fit the authors feet for testing, they are approximately a size 47 European. As a result, the evaluated solution might not work as well or even be applicable on smaller shoe sizes.

This product is legally considered by The Swedish Transport Agency as a bicycle when conveyed on public roads. By law, the vehicle must then be equipped with headlights, reflectors and a bell, as well as follow regulations about speed and power [2]. While the possibility of complying with the regulations to make the shoes legal on the public roads was considered, this was not to be part of the project scope. The shoes were tested and developed on closed tracks.

In order to evaluate the purpose regarding the technological readiness, all electrical components used were readily available on the market.

To make this concept into a complete product for the market, both left and right shoe designs needed to be developed. Only the right shoe carries the drivetrain and electronics, as this is the driving shoe. The only purpose of the left shoe is to support the users balance. Because of this, the right shoe is mainly considered for this thesis, whilst the left shoe received greatly reduced time invested in its development.

1.4 Method

As a method of answering the questions in section 1.2 Purpose, a prototype was constructed that can be strapped onto a shoe. Firstly, in order to decide which driveline components will be utilized, a simulation that calculates theoretical motor power and battery characteristics for the defined use case was written in MATLAB. Furthermore, 3D models were created in Solid Edge of said components, in addition to the structural components. ANSYS was used to analyze the strength and solidity of the structural load bearing components.

When the theoretical construction was deemed sufficient to withstand the use case, the physical prototype was built. For the prototype, materials that are readily available and easily malleable were utilized. This mainly includes steel, wood, and 3D printed plastic. As the last step of the construction, the microcomputers were programmed to interpret the user input and send a corresponding power output signal to the driveline.

Finally, experiments were conducted with the prototype for the regular use cases, which is set out to answer above mentioned questions.

Chapter 2

Theory

This chapter introduces the specific theoretical information needed to understand the aspects surrounding this project. It for example includes how different components function, explanations of some methods, and what alternative solutions exist on the market.

2.1 Battery

The energy needed to propel the shoes will be stored in a battery, this battery can be created in different ways in order to achieve the desired performance.

There are several types of battery technologies on the market, utilizing different chemicals to store energy. Lead acid battery, PB, is the most widely used battery for industrial electric vehicles [3]. However, other modern technologies such as Lithium-ion, Li-ion, and lithium-ion polymer, LiPo, offer greater specific power and specific energy [3]. This means that a battery can be smaller and lighter while offering the same performance, see Table 2.1.

Table 2.1. Specifications of different battery technologies [3]

Battery technology	Specific energy [Wh/kg]	Specific Power [W/kg]	Nominal voltage [V]
Pb	25-30	80-300	2.1
Li-ion	60-190	80-10000	3.6
LiPo	120-150	80-2000	3.7

A battery consists of at least one battery cell, but more cells can be used in series or parallel with each other to create a larger battery. When cells are in series, the potential is increased with every added cell. The nominal voltage of a LiPo-cell is 3.7 V, as seen in Table 2.1. If two of these cells are connected in series, the result would be a 7.4 V battery. However, if the cells where to be connected parallel to

one another, the current per cell would effectively be halved. The resulting battery would still be 3.7 V but the cells would drain at half the speed, which leads to an increase in battery capacity [4]. The cells are rated with max capacity, Q, and relative safe rate of discharge, C. The discharge rate, I, can be calculated with Equation 2.1.

$$I = Q \cdot C \tag{2.1}$$

Each cell in the battery has a cutoff voltage, and this is the voltage at which the cell is considered empty. For LiPo the cutoff voltage is 3.0-3.3 V/cell under normal load and 2.7 V/cell under heavy loads [5]. The usable voltage in a battery cell is the difference between max charge and the cut off voltage. LiPo batteries can sometimes be unstable when used incorrectly, it is therefore important that the batteries are not strained above their ratings, as noted earlier.

When a LiPo battery is being charged the individual cells must be held at level charge toward one another [6]. For this purpose, a specific battery charger has to be used. It connects to the poles on each cell and makes sure all of the cells keep level during the charge process.

2.2 Motor

Electric motors that are applicable with the current constrains consist of two main classes: brushed direct current, DC, and brushless direct current, BLDC [7]. Additionally, Harrington and Kroninger [7], states the following information in this paragraph: The main differentiating factor between these types are the brushes, which create a conductive contact patch between the rotating part and the static part of the motor. They exist in order to start and control the motor when at speed, simply by changing the input voltage. On the downside, having contact between static and moving parts creates friction and wear, which limits maximum power output and lifespan. Removing the need for this contact patch gives us brushless motors. The lack of contact between moving parts can result in this type having higher efficiency, speed, and torque. The BLDC motors functions by having several coils that can be controlled individually. These coils will be activated in pairs at precise time intervals with regards to the rotational speed of the motor, see Figure 2.1.

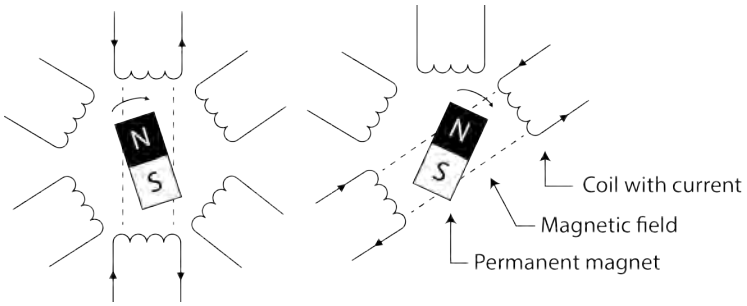

Figure 2.1. Principles of how a BLDC electric motor function. Created in Adobe Illustrator.

Because of the required preciseness, BLDC motors are commonly equipped with a hall sensor, in order to acquire the position of the magnet. The sensor works by altering its conductivity in proportion to the strength and direction of the magnetic field created by the magnet inside the motor [8].

2.3 Electric Speed Controller

The output from the hall sensor, as well as input from the user, is interpreted by an electric speed controller, ESC. According to the input from the user and the signal from the hall sensor, the ESC regulates the phase and voltage over the coils to drive the motor accordingly [7].

A common and powerful type of ESC is the so called VESC. VESC is an open-source project that aims to create a blueprint for motor control, containing firmware, software, and hardware [9]. Because of the projects open-source nature, hardware can be purchased from a range of different manufacturers. This hardware can then be programmed with the VESC Tool [10], and loaded with corresponding firmware to be configured properly for the use case of the motor.

2.4 User input

The goal regarding user input is to control the shoes without using a handheld remote. Since the sensors will be incorporated inside of the design, the choices become limited. The applicable alternatives include some type of pressure sensitivity or positioning sensors.

Safety is of great importance in this type of application, which requires having a reliable user input method. Using positioning sensors for control can intervene with this. In order to stay in balance, the user will need to freely move about their feet, which the positioning sensor will interpret as an input. Instead, using a sensor type called load cells is an accurate and reliable way of measuring input, if implemented properly [11].

Based on Schmidt [12], these typically consist of a strain gauge mounted on a spring element. The strain gauge is a type of elastic film, lined with electric wire. When the spring element compresses or elongates under load, the electric wire in the film does the same. This results in a change in conductivity over the strain gauge, responding to the force.

A way to measure this chance in conductivity is to implement a Wheatstone bridge, since it is well suited for measuring small changes in conductivity [13]. A schematic diagram of a typical Wheatstone bridge is shown in Figure 2.2. Here, R_1 and R_2 can represent the load cell, whilst R_3 and R_4 represent regular static resistors, or another load cell.

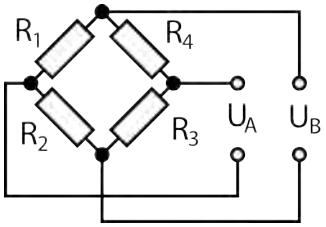

Figure 2.2. Schematic of a Wheatstone bridge. Created in Adobe Illustrator.

2.5 Micro Computer

To control the behavior of the motor in a way that follows the instructions given by the user input, a micro computer will be part of the construction. A micro computer is small and often inexpensive computer equipped with a microprocessor, a memory, and input/output, I/O, pins to control and measure electrical signals [14].

A company called Arduino manufactures these types of micro computers, in addition to providing an open-source electronics platform. Their product range includes the *Arduino UNO* and the *Aduino NANO* micro computers, see Table 2.2.

Table 2.2. Two Micro Computers from Arduino [3].

Micro computer, Arduino	UNO	NANO
Microcontroller	ATmega328P	ATmega328P
Clock speed [MHz]	16	16
Flash memory [KB]	32	32
Digital I/O pins	14 (6 PWM)	22 (6 PWM)
Analog input pins	6	8
Length [mm]	68.6	45
Width [mm]	53.4	18
Weight [g]	25	7

Based on this projects requirements, the smaller version, *Arduino NANO* was selected. This micro computer has a number of pins, some marked with Analog input and some with Digital I/O. The Analog input pins are used for measuring analog signals between 0 V to the operational voltage 3.3-5.0 V. The on-board micro controller translates the analog signal to a digital signal, with the use of an analog-to-digital converter. The converted digital signal consists of a 10-bit value that describes the strength of the input signal [15].

The Digital I/O ports can be used in a similar fashion when declared as inputs. However, the value after conversion in this configuration is only stored as a digital high or low, depending on the signal in question. This means that no interval of voltage can be measured, simply on or off. The Digital I/O pins can also be declared as outputs. In this configuration they output a high or low voltage [16].

2.6 Pulse Modulation

To produce an output signal between the low and high range of 0-5 V, a technique called Pulse-width Modulation, PWM, can be used. PWM utilizes voltage pulses with varying time length to simulate specific voltages [17]. To achieve a signal with the voltage of 2 V, the 5 V pulse is active for 40 percent of each time window. The windows are small, meaning the simulated signal is similar to an analog 2 V signal, see Figure 2.3.

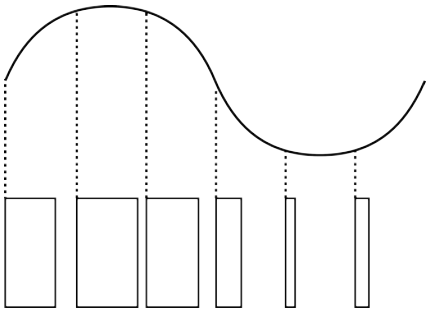

Figure 2.3. Illustration of Pulse-width Modulation. Created in Adobe Illustrator.

Pulse-position Modulation, PPM, is a similar technique that is more useful when sending signals, rather than directly powering the target component. PPM works by sending a pulse somewhere in a predefined time window. Sending the pulse in the beginning or towards the end of the window determines the strength of the signal [17].

Chapter 3

Demonstrator

This chapter includes the reasoning behind and the building of a prototype. It defines all the components and explains the written code. Figure 3.1 shows the completed right shoe prototype. Also see Appendix A.3, Prototype, for more images.

Figure 3.1. Image of the built prototype. Taken by authors.

3.1 Driveline

The driveline is the collection of components that together create the driving force that propels the prototype forward. In this section these components are selected and justified.

3.1.1 Calculations and Simulation

To create a decision basis for choosing driveline components, a simulation in MATLAB was written. See Appendix C.1 for the complete code. Throughout the simulations, all parameters except battery voltage and angle of the slope were kept constant. With this setup, the capacity and discharge rate of the battery could be

computed, as well as the required motor power output. All constant parameters are defined and given numerical values continuously throughout the text, whilst the variable parameters values are presented at the end of this section in Table 3.1.

The main part of the simulation is a power equilibrium, according to Equation 3.5, shown later in this section. In order to set it up, all forces acting on the user and its shoes needed to be calculated first. These consist of:

Rolling resistance of the bearings:

$$F_{bea} = \mu_f F_{load} \tag{3.1}$$

Where $\mu_f = 0.0015$ is the coefficient of friction inside the bearing, which corresponds to a deep grove ball bearing [18]. The F_{load} is the total vertical force acting on the bearing. This was set to $F_{load} \approx 850\ N$, as this represents a person weighing 85 kg.

Rolling resistance of the ground-wheel contact:

$$F_{roll} = C_{rr} F_{load} \tag{3.2}$$

Where $C_{rr} = 0.003$ is the coefficient of rolling resistance between the ground and wheel [19]. The F_{load} is defined equally as mentioned above.

Air resistance is derived from:

$$F_{air} = \frac{1}{2} C \rho A v^2 \tag{3.3}$$

Where $C = 1.2$ is the coefficient of aerodynamic resistance for a person standing, facing the direction of travel [20]. According to section 1.2 Purpose, the speed is kept constant at $v = 15/3.6\ m/s$. The projected area in the direction of travel was set to $A = 0.75\ m^2$ [21]. The air density was set to $\rho = 1.225\ kg/m^3$.

Gravity is derived from:

$$F_g = mgsin(\theta) \tag{3.4}$$

Where $m = 85\ kg$ is the mass of the person with shoes, $g = 9.82\ m/s^2$ is the gravitational acceleration, and θ is the variable angle of the slope.

All of the forces mentioned above were combined into the power equilibrium according to Equation 3.5.

$$W_{motor} = v(F_{bea} + F_g + F_{air} + F_{roll}) \tag{3.5}$$

W_{motor} is the total power output from the electrical motor. From this, the total energy usage, E, could be calculated.

$$E = W_{motor} \frac{d}{v} \tag{3.6}$$

Where d/v is the distance travelled, divided by average speed, which gives total time. Once again, these are gathered from section 1.2 Purpose, which gives $d = 3\ km$ and $v = 15/3.6\ m/s$. Using this result, the battery characteristics were calculated.

$$Q = \frac{E}{3.6U} \tag{3.7}$$

The nominal voltage over the battery, U is variable throughout the calculation, to test different battery configurations. This gives Q, which is the required battery capacity in the case of no losses in the circuit. Since there are losses in any physical circuit, Q is divided with a loss constant k, to calculate the real required battery capacity Q_{batt}.

$$Q_{batt} = \frac{Q}{k} \tag{3.8}$$

Where k was set to 0.7. Continuing from this result, the discharge rate for the battery, C, was calculated.

$$C = \frac{W_{motor}}{UQ_{batt}} \tag{3.9}$$

Finally, the maximum continuous current from the battery, I_{max}, was calculated.

$$I_{max} = \frac{W_{motor}}{Uk} \tag{3.10}$$

All calculations above were done for three different battery voltages, and two different slope angles. The first evaluation was with a slight slope of $\theta = 1^o$, in order to calculate the required battery capacity. The results are given in the first part of Table 3.1. The second evaluation was done to calculate at a slope of $\theta = 10^o$. This represents maximum power, which in turn gives discharge rate and maximum continuous current. Battery capacity was kept the same as in the first evaluation, as this use case only is applicable momentarily in regular use. The results are given in the second part of Table 3.1.

Table 3.1. Variable input parameters and their respective results for driveline simulations. Calculated by MATLAB.

Variable	Designation	4 cell	5 cell	6 cell	Unit
Battery voltage	U	14.8	18.5	22.2	[V]
Battery Capacity	Q	3200	2600	2200	[mAh]
Discarge rate	C	19.9	19.6	19.3	[1/h]
Maximum Current	I_{max}	63.7	50.9	42.4	[A]
Motor Power	W_{motor}	659.5	659.5	659.5	[W]

In conclusion, the simulations showed that a six cell, six series battery is preferred, because of the significantly lowered maximum current compared to the lower cell counts. Having more cells would lower I_{max} even further, but generally having more cells results in a larger battery. For this application six cells were deemed to be the maximum applicable size.

Moreover, a visual simulation of the acceleration was written in the programming language ACUMEN, see Appendix C.2.

3.1.2 Battery

In accordance with the simulations, the selected battery for this project is a six cell, six series, LiPo-battery from Zippy Technology, see Figure 3.2. The battery has a capacity of 3000 mAh and can discharge at a rate of 20 C, with a burst discharge of 40 C. This means that the maximum continuous current, according to Equation 2.1, is 60 A, which is adequate for this project.

Figure 3.2. LiPo battery, Zippy. Taken by authors

3.1.3 Motor

Flipsky Technology produces a BLDC motor called the 5065, see Figure 3.3. The motor is made for 11.1 V to 29.6 V, has a max current of 80 A, and a maximum power output of 1550 W. The motor is particularly interesting because of the relatively low rotation per voltage number of 270 KV. This translates to a powerful motor at low rotation speeds, which is useful when accelerating a larger mass, such as a person.

Figure 3.3. Brushless electric motor, 5065, Flipsky Technology [22].

An internal Hall effect sensor, see section 2.2 Motor, is mounted inside the motor. It is connected to the electric speed controller, which in turn can measure the current rotational position of the motor and decide which coils to activate.

3.1.4 Electric Speed Controller

The chosen speed controller is a VESC, as discussed in section 2.3 Electric Speed Controller. This model is produced by Flipsky Technology, see Figure 3.4. It is rated for use of up to 60 V and 50 A continuous current, with bursts of up to 150 A, all while being passively cooled through on-board mounted heatsinks. This VESC is relatively small, and only measures 67x39x18.3 mm, which is important because of the space constraints of this project.

The VESC is equipped with a battery eliminator circuit, BEC. When the VESC is directly connected to the high voltage battery, it can feed 5 V at a maximum of 1.5 A through a secondary output. The low voltage components in this project, including the Arduino NANO, can subsequently be powered from this output. As the name suggest, the BEC eliminates the need for a second battery to power these components.

Figure 3.4. Electric Speed Controller, Mini FSESC4.20 50A, Flipsky Technology [22].

3.2 Structural Design

The above chosen components were to be mounted together in a manner that still allows the shoes to be walked with for shorter distances, according to section 1.2 Purpose. Several prototype sketches were drawn and evaluated with the research questions in mind. Preferably, the wheel(s) should not touch the ground when walking, which ultimately lead to a design that mounts the components below the users regular shoes.

The chosen configuration for the driving shoe is to have a single wheel at the rear of the construction, and a large flat surface at the front. This allows the shoes to be driven while standing on the heel, and walked with when kept parallel to the ground. To achieve this, the structural design is divided into two main parts: the front housing and the rear frame. The front housing is the enclosure for the battery,

the Arduino NANO, the load amplification board (see section 3.3 User Input), as well as the electronic speed controller.

The rear frame carries the motor, which drives the wheel through friction contact. As the motor is an outrunner, meaning the outer chassis is rotating as well as the axle, this type of design is possible. The motor is consequently mounted to an extension with elongated bolt clearances to achieve the correct fitment. If the motor is mounted too far away from the wheel, the bolts can simply be loosened, and the motor can be moved closer.

The front and rear assemblies are both mounted to a plate that resembles the size and shape of a shoe. On the top of this plate, straps are mounted that wraps around the users shoes to keep them from sliding off. See Figure 3.5 for an exploded view of the construction.

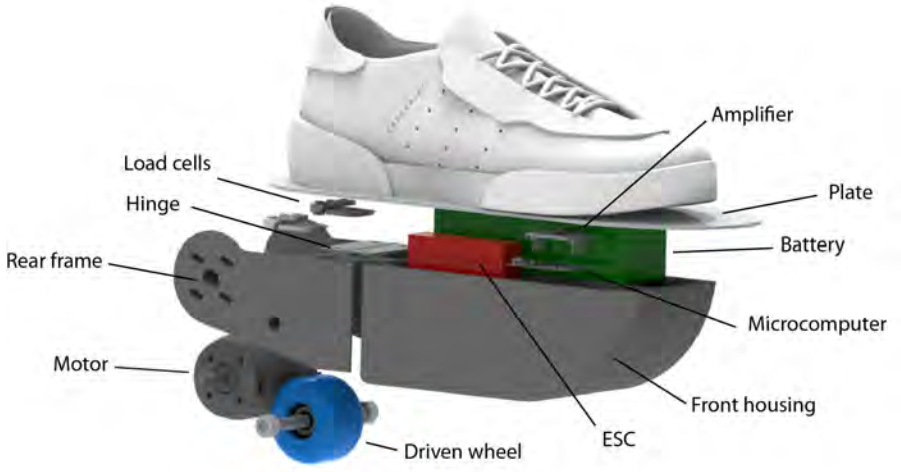

Figure 3.5. Exploded view of design. Created in Solid Edge.

3.3 User Input

With this type of design, the user will stand on the heel of the driving shoe while rolling. Because of this, it was chosen to situate the load cells between the rear wheel and heel of the shoes. The user can then input the desired motor power by simply shifting more weight over to the driving shoe, which is the right one. This is analog to how you would drive a car, as the accelerator pedal is to the right, making the shoes easier to control for a beginner.

To measure this load accurately the whole rear frame is mounted on a hinge [23]. Two load cells are then mounted on top of the rear frame, to be squeezed down by the top plate when pressure is applied by the user. Whilst one load cell of the

selected type can measure up to 50 kg, and has a max weight of 75 kg, see Figure 3.6, two cells connected in this configuration can accurately measure in the range 0-100 kg. This means that the cells on this prototype can take loads of up to 150 kg and measure up to 100 kg, which is sufficient for this project. They were connected in a Wheatstone bridge in order to accurately read the load on the cells, see section 2.4 User Input.

Figure 3.6. Generic Load Cell. Max weight 75 kg [24].

The load cells required fine measurements in order to determine the current load. This is handled by an amplification board, HX711, see Figure 3.7. The board runs a 5 V current through the load cells, and measures changes in conductivity over the Wheatstone bridge. An amplified signal is then sent to the Arduino NANO to be interpreted. The full wiring diagram can be found in Appendix A.1.

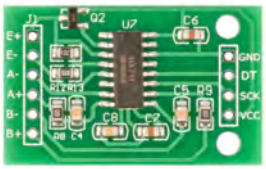

Figure 3.7. Amplification board for load cells [25].

3.4 Programming

This section include the code and configuration necessary to operate the prototype. The Arduino NANO and the electronic speed controller are both targeted.

3.4.1 Code

One of the main goals for this concept was to drive the motor when the user applies pressure onto the rear wheel. The microcomputer is responsible for the task of reading the input signal from the two load cells, and translating it into the desired output signal, which is sent to the electric speed controller. The first phase of the program initializes the communication with the ESC, and applies the correct

calibration for the load cells. To interpret when the motor should be driven, pressure limits are defined. The lower limit refers to the minimum pressure required to start the motor, and the upper limit refers to the pressure required to spin the motor at full speed. It is of course important that the lower limit is set above zero, not to accidentally start the motor. See Figure 3.8 for a visualization of the logic in the program.

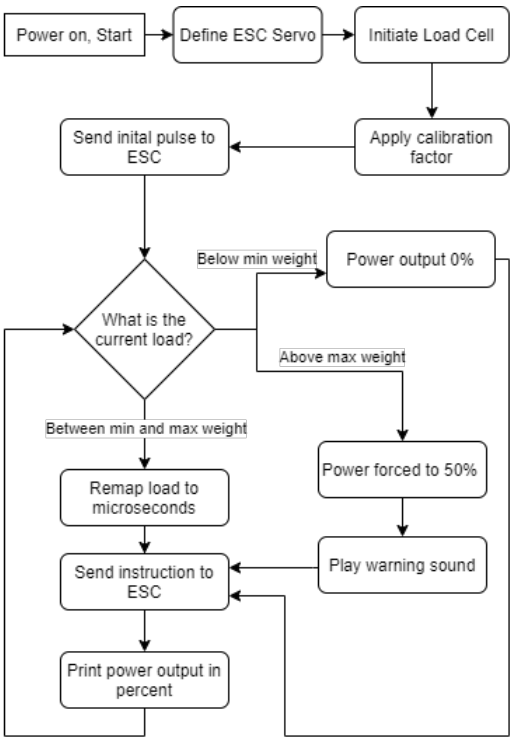

Figure 3.8. Code, Flowchart. Created in draw.io.

3.4.2 Configuration of Electric Speed Controller

VESC Tool [10] was used to program the ESC, to interpret the input and produce the output correctly.

In order to control the motor efficiently, its properties need to be precisely defined. This could be done automatically with a test run feature through the VESC Tool software.

The input parameters were instead configured manually. The Arduino microcomputer outputs the desired power signal through PPM, see section 2.5 Micro Computer, with a timing of 1 ms to 2 ms. The ESC was configured accordingly. In addition, a three percent dead zone was added, to mitigate the effect of noise in the signal.

Furthermore, as discussed in section 2.1 Battery, the LiPo-cells should not be discharged below 3-3.3 V. Because of this, a soft-stop was configured for when the battery voltage drops below 18.6 V, since it has 6 cells in series. As a result, the battery cells will not be damaged as the device will simply slow to a halt instead.

3.5 Evaluation of Materials and Stress

Due to the nature of this design, all parts need to be able to support the full weight of the user, see F_{load} in section 3.1.1 Calculations and Simulation. When rolling, the rear wheel assembly supports the full weight of the user, and when stationary the front housing supports the same weight. This raised some concerns about the rigidness and strength of the design and materials. To make sure the proper dimensions and materials were utilized, a stress analysis was conducted.

Both the front housing and rear frame were 3D-printed using PLA-plastic. This made it possible to accurately create parts with predefined dimensions that fit the purchased components well. The top plate connecting these two was produced from plywood, because of its malleability.

As shown in Figure 3.9, a spike in stress was situated on the connecting part above the rear wheel, where the load cells are situated. This area was strengthened with the use of a steel plate, to prevent it from deforming and breaking. See Figure A.2 and Figure A.3 in Appendix for further analysis of said steel plate, and front housing.

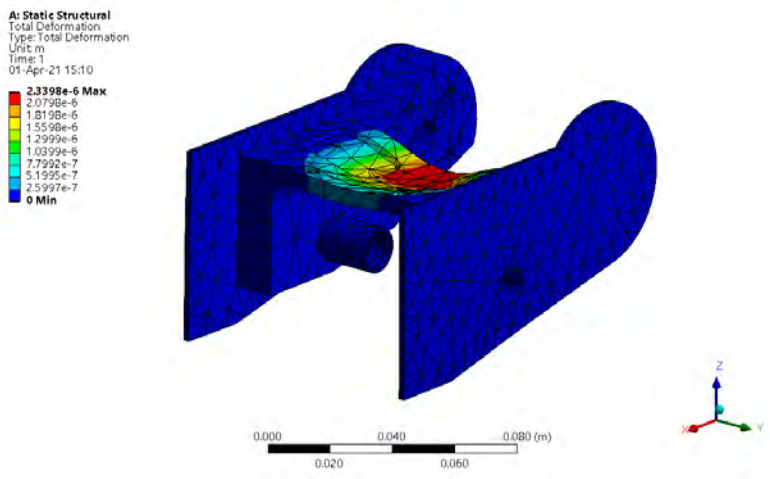

Figure 3.9. Deformation, Rear assembly. Created in ANSYS.

Chapter 4

Experiments

This chapter includes the results from all the conducted experiments, done with the built prototype.

4.1 Ease of use

When the prototype is used, the user controls the speed by moving more or less weight onto the right foot, as discussed in section 3.3 User Input. To make the prototype as user-friendly as possible, the two weight limits to achieve maximum and minimum power output were altered. These limits proved to be of great importance as the user experience degraded rapidly when not configured properly.

The results were a minimum limit of 3 kg and maximum limit of 50 kg, with a strictly linear correlation between input and output within the interval. The weight limits correspond to 3.75 % and 62.5 % of the users weight, which proved to be a desirable interval as the lower limit prevents the prototype from starting by accident, without the user having to place an unnecessary large amount of weight during a start. The higher limit resulted in a good compromise between safety and control. Having the correlation being linear made the power output feel the most intuitive.

As a result of handling input with the right foot, being able to easily balance on the wheel is of great importance. The current configuration uses a sole skateboard wheel, which made balancing difficult, as it is only 24 mm wide at the contact patch.

4.2 Range

The range test was conducted on a closed test track where the authors drove the prototype until a fully charged battery was depleted. The test subject was in accordance with the scope of the project, see 1.3 Scope, a person weighing approximately 85kg. The measuring was done by the use of Google Maps [26].

The total travel distance measured, $d \approx 4.2\ km$.

Note that this experiment was dependent on a multitude of factors that could not be easily controlled. The tarmac, angle of the road, and the wind for example, could have impacted this test significantly. However, this test highlights that the desired range of 3 km is within reach.

4.3 Speed

Several speed tests were conducted, and the results proved that the desired top speed of 15 km/h was reached. The prototype continued to accelerate beyond the desired top speed and a conclusion can be made: the top speed is beyond the smallest acceptable target of 15 km/h. To ensure that no accidents occurred during testing, no maximum speed test was conducted as this was determined to be a risk factor.

The results were obtained by measuring the time it took to travel a previously measured distance, and the speed was then calculated, see Table 4.1.

Table 4.1. Data from speed test. Measured by authors

	Test 1	Test 2	Test 3	Unit
Travel distance	10	10	10	m
Time	2.2	2.5	1.9	s
Calculated speed	16.3	14.4	18.9	km/h

Chapter 5

Discussion and Conclusion

This chapter discusses and draws conclusions from all aspects of the project.

5.1 Discussion

The final prototype measures 80 mm in height, and this is one of the main improvement areas for the design. To make the product more useful to a potential customer, one the main features was to allow the user to walking shorter distances. While this is possible with the current prototype, it is not ideal. The primary reason for the height derives from the use of load cells with a hinge, which added about 25 mm in total. Three different things could be done in order to lessen this problem. Firstly, another structural design could be used, that does not locate the load cells directly above the rear wheel. This could on the other hand create problems with the load not being read correctly, as the user will place the weight directly through the rear wheel. Secondly, a smaller wheel size can be chosen. For the prototype, a 51 mm in diameter skateboard wheel was used, which is made from firm Polyurethane rubber. Lowering this diameter could impact ride quality, which already was quite stiff. Because of this, a softer material would need to be chosen, and ride quality would need to be assessed if a smaller diameter wheel is utilized instead. Lastly you could change to a different input method if both height and ride quality are not achieved satisfactory.

If the height was to be reduced, problems would arise in the front housing, as the chosen battery's height, see 2.1 Battery, limits the design in this regard. A custom battery could be wielded to fit the space requirements better. The battery capacity could also be reduced as the experiments showed that the range was slightly longer than required, see section 4 Experiments.

Furthermore, the load cells contribute to another difficulty as the input method makes it hard to implement a reliable brake. The current solution was to use friction between the front housing and the ground. This solution could be unreliable as the usable friction differs greatly between weather conditions and terrain. It is possible to use the electric motor to brake. However, with the load input method, the user would have to release pressure from the breaking wheel in order to stop. This would of course lead to lessened usable friction force between the braking wheel and the road, something that is not favorable. The breaking mechanism could instead be incorporated into the left shoe, which would then naturally slow you down as transfer the weight from the load cells.

According to the calculations done in section 3.1.1 Calculations and Simulation, the maximum needed motor power was 659.5 W. This is not in line with the chosen motor, which has a maximum output of 1550 W, see section 2.2 Motor. This is because no motor on the market perfectly fit the requirements. Having a lower maximum power output could also give benefits to the dimensions of the battery and ESC, as smaller and less power capable variants could be chosen. Simultaneously, a hub motor would have been preferable as this would remove the need of having a rear wheel and motor combination. This hub motor could also preferably be wider than the current rear wheel, because of the balancing issues mentioned in section 4.1 Ease of use.

Another potential improvement is the cooling in the front housing. Inside the plastic shell, the battery and the electric speed controller emits heat. As no thermal data was gathered during the long range testing, a potential problem cannot be determined accurately. However, while conducting the tests no significant heat developments were discovered as an implication of using the prototype as intended.

5.2 Conclusion

The final prototype is a shoe mountable electrically propelled personal transportation vehicle, that can transport a person further than 3 km with a top speed above 15 km/h as demonstrated through testing.

A good way to configure the battery and motor is by selecting a six series, one parallel, lithium-ion polymer battery and a brushless electric motor capable of a power output above 659.5 W.

Mounting a driveline onto a regular pair of shoes is best done by placing the components underneath the shoes, as this allows them to be uniformly configured and allows for walking.

A good way of controlling the speed without using an external remote control is by the use of load cells. This is done by measuring weight distributions between the users feet and hence determining the desired speed.

In order to answer the questions stated in section 1.2 Purpose, the prototype ended up being larger than desired with a non-optimal brake system. Future work could improve upon this prototype, and with more compact battery technology this concept could potentially develop into a market-ready product.

Chapter 6

Further work

If this concept is to be adapted into a complete product for the market, several aspects is in need of further work. Naturally, all aspect of the prototype build can be fine-tuned to some extent.

In order to apply with the current legal regulations, several features such as a bell, lights and power limit should be added for use in public areas.

Furthermore, some ease of use features should be implemented, such as a power button and an emergency shut off. More functionality surrounding the battery could as well be implemented. For example an external charging port, and some type of display showing the current remaining energy percentage.

Finally, the non-driven left shoe should be developed in conjunction with the driven right shoe, as the whole concept is greatly dependent on the left for balancing and general ease of use, possibly including some braking mechanism as mentioned in section 5.1 Discussion.

Bibliography

[1] M. Svegander,
"The bike and scootersharing telematics market – 2nd edition",
Berg Insight, Report, 2020. [Online]. Available:
http://www.berginsight.com/ShowReport.aspx?m_m=3&id=333.

[2] "Cykel", *Transportstyrelsen*, Aug. 2013, (visited on 2021-01-28).
[Online]. Available: https://www.transportstyrelsen.se/sv/vagtrafik/Fordon/Fordonsregler/Cykel/.

[3] P. Van den Bossche, F. Vergels, J. Van Mierlo, J. Matheys, and W. Van Autenboer, "Subat: An assessment of sustainable battery technology", *Journal of Power Sources*, vol. 162, no. 2, pp. 913–919, 2006, Special issue including selected papers from the International Power Sources Symposium 2005 together with regular papers, ISSN: 0378-7753.
DOI: https://doi.org/10.1016/j.jpowsour.2005.07.039.
[Online]. Available: https://www.sciencedirect.com/science/article/pii/S0378775305008761.

[4] J. Zhang, S. Ci, H. Sharif, and M. Alahmad, "Modeling discharge behavior of multicell battery", *IEEE Transactions on Energy Conversion*, vol. 25, no. 4, pp. 1133–1141, 2010. DOI: 10.1109/TEC.2010.2048904.

[5] I. Buchmann, "Bu-501: Basics about discharging",
2019, (visited on 2021-02-10).
[Online]. Available: https://batteryuniversity.com/index.php/learn/article/discharge_methods.

[6] Y. Barsukov, "Battery cell balancing: What to balance and how",
Texas Instruments, pp. 1–8, 2018.
[Online]. Available: http://www.amarketplaceofideas.com/wp-content/uploads/2018/09/Topic20220-20Battery20Cell20Balancing20-20What20to20Balance20and20How1.pdf.

[7] A. M. Harrington and C. Kroninger,
"Characterization of small dc brushed and brushless motors",
Army Research Laboratory, Aberdeen Proving Ground, Vehicle Technology

Directorate, Report, Mar. 2013. [Online]. Available: https://apps.dtic.mil/sti/citations/ADA577582.

[8] M. E. Huvén, "Electric motor control", Master's Thesis, Royal Institute of Technology, Oct. 2010. [Online]. Available: http://urn.kb.se/resolve?urn=urn:nbn:se:kth:diva-49587.

[9] B. Vedder, "Vesc", *VESC Project*, (visited on 2021-03-10). [Online]. Available: https://vesc-project.com/.

[10] "Vesc tool", *VESC Project*, (visited on 2021-03-10). [Online]. Available: https://vesc-project.com/vesc_tool.

[11] I. Muller, R. M. de Brito, C. E. Pereira, and V. Brusamarello, "Load cells in force sensing analysis – theory and a novel application", *IEEE Instrumentation Measurement Magazine*, vol. 13, no. 1, pp. 15–19, 2010. DOI: 10.1109/MIM.2010.5399212.

[12] S. Schmidt, "What is a load cell? how does a load cell work?", *HBM*, (visited on 2021-02-10). [Online]. Available: https://www.hbm.com/en/6768/what-is-a-load-cell-and-how-does-a-load-cell-work/.

[13] K. Hoffman, "Applying the wheatstone bridge circuit", *Hottinger Baldwin Messtechnik GMBH, Darmstadt*, 1986.

[14] D. Ibrahim, "Pic32 microcontrollers and the digilent chipkit, chapter 1 - microcomputer systems", *Newnes*, pp. 1–14, 2015. DOI: https://doi.org/10.1016/B978-0-08-099934-0.00001-6. [Online]. Available: https://www.sciencedirect.com/science/article/pii/B9780080999340000016.

[15] "Analogread()", *Arduino*, (visited on 2021-02-11). [Online]. Available: https://www.arduino.cc/reference/en/language/functions/analog-io/analogread/.

[16] "Digitalwrite()", *Arduino*, (visited on 2021-02-11). [Online]. Available: https://www.arduino.cc/reference/en/language/functions/digital-io/digitalwrite/.

[17] Y. Fan and R. J. Green, "Comparison of pulse position modulation and pulse width modulation for application in optical communications", *Optical Engineering*, vol. 46, no. 6, pp. 1–7, 2007. DOI: 10.1117/1.2746010. [Online]. Available: https://doi.org/10.1117/1.2746010.

[18] "Maskinelement. handbok", *Institutionen för maskinkonstruktion, Kungl. tekniska högskolan*, vol. 2008 års uppl.. 2008.

[19] D. Lippert and J. Spektor, "Rolling resistance and industrial wheels", *Hamilton*, vol. Hamilton White paper No.11, 2013. [Online]. Available: https://www.mhi.org/media/members/14220/130101690137732025.pdf.

[20] A. S. Al-Obaidi and M. Koo, "Calculation of aerodynamic drag of human being in various positions", pp. 99–100, Jul. 2013, Conference Paper. [Online]. Available: https://www.researchgate.net/publication/321866543_Calculation_of_Aerodynamic_Drag_of_Human_Being_in_Various_Positions.

[21] J. J.Swearingen and E. B. McFadden, "Studies of air loads on man", *Federal Aviation Agency, Oklahoma*, Jul. 1964. [Online]. Available: https://www.faa.gov/data_research/research/med_humanfacs/oamtechreports/1960s/media/AM63-09.pdf.

[22] *Flipsky Technology*, (visited on 2021-04-28). [Online]. Available: https://flipsky.net/.

[23] J. Andersson and R. Höglund, "Electric load driven longboard", Bachelor's Thesis, Royal Institute of Technology, Aug. 2020. [Online]. Available: http://urn.kb.se/resolve?urn=urn:nbn:se:kth:diva-279809.

[24] *Electrokit Sweden AB*, (visited on 2021-04-28). [Online]. Available: https://www.electrokit.com/produkt/lastcell-50kg/.

[25] "Hx711", *Avia Semiconductor*, (visited on 2021-04-28). [Online]. Available: http://en.aviaic.com/detail/730856.html.

[26] "Google maps", *Google*, (visited on 2021-04-28). [Online]. Available: https://www.google.com/maps.

Appendix A

Figures

A.1 Wiring Diagrams

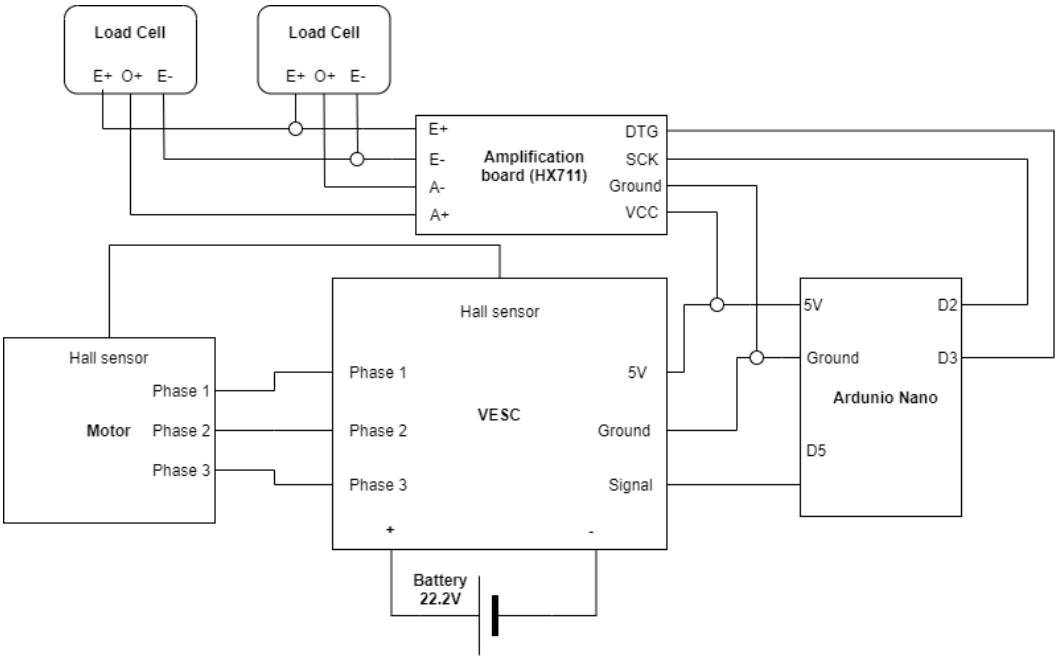

Figure A.1. Wiring Diagram. Created in draw.io.

A.2 Stress Analysis

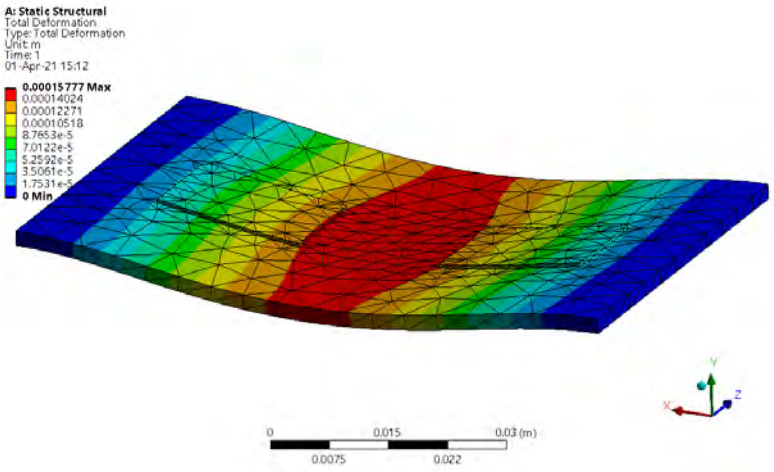

Figure A.2. Deformation, Steel plate. Created in ANSYS.

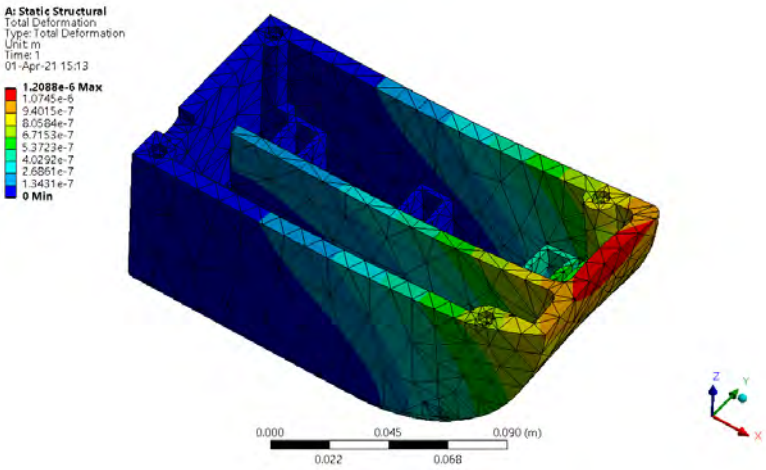

Figure A.3. Deformation, Front housing. Created in ANSYS.

A.3 Prototype

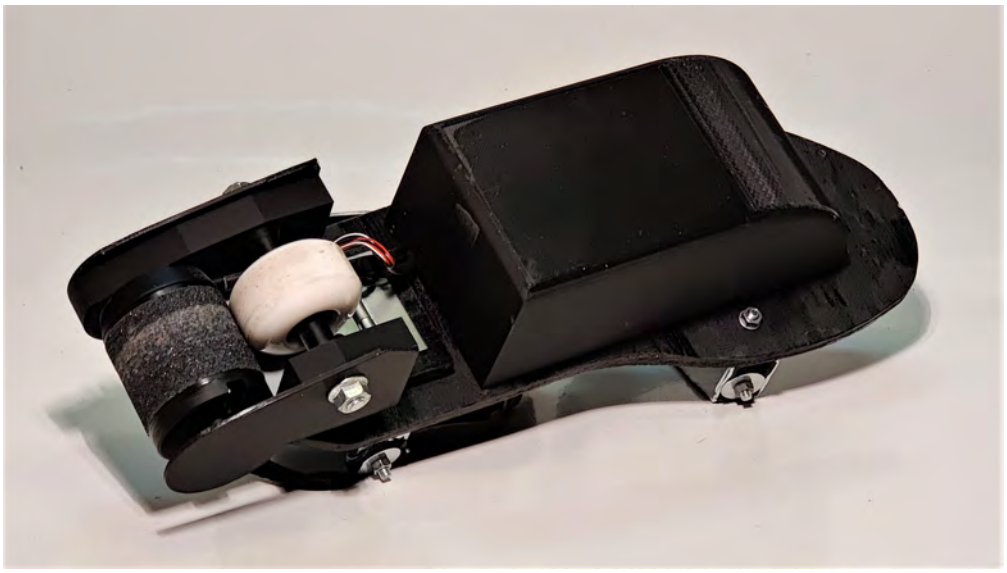

Figure A.4. Image of prototype, from below. Taken by authors.

Figure A.5. Image of both right and left prototype. Taken by authors.

Figure A.6. Image of prototype, with a shoe. Taken by authors.

Figure A.7. Image of opened prototype. Taken by authors.

Appendix B

Arduino Code

```
1  //Electric Self Propelled Shoe
2  //Bachelors Thesis MF133X
3  //Date: 2021 02
4  //Authors: David Stridfeldt, Viktor Karefjard
5  //Description: Code running on Arduino Nano.
6  //Translates load measurements into
7  //instructions for electric speed controller.
8
9
10 //Import the required libraries
11 #include <HX711.h>
12 #include <Servo.h>
13
14 //Define Electric Speed Controller as a Servo.
15 Servo esc;
16
17 //Initiate Load Cell, HX711.
18 HX711 scale;
19
20 //Define the calibrationfactor to mesure accurate weight with the load cells.
21 //And define the inital load as zero.
22 #define calibrationFactor 47000.0
23 float currentLoad = 0;
24
25 //Defining pin layout on the Arduino.
26 const int LoadSCKPin = 2;
27 const int LoadDOutPin = 3;
28 const int speakerPin = 4;
29 const int VescOutputPin = 5;
30
31 //Defining the weight in kg required to ouput min/max power
32 //from the motor.
33 const int MaxSpeedWeight = 75; //kg --> 100% motor power.
34 const int MinSpeedWeight = 15; //kg --> 0% motor power.
35 const int errorIntervall = 25; //kg --> Diff between max speed and load ...
       warning
36
37 //Setup, Runs at start only
38 void setup() {
39
40   Serial.begin(9600); //Turn on the serial monitor
41                       //to see current values on screen when testing.
```

```
42
43   pinMode(speakerPin, OUTPUT); //Set the speaker pin as output
44
45   //Setup the Electric Speed Contoller, (ESC).
46   esc.attach(VescOutputPin); //Initiate ESC as servo on the currect pin.
47   esc.writeMicroseconds(1500); //Initiate pulse to ESC.
48
49
50
51   //Starting the load cell scale
52   Serial.println("SCALE STARTED: ");
53   scale.begin(LoadDOutPin, LoadSCKPin); //Start ESC.
54   scale.set_scale(calibrationFactor); //Apply the scale calibration factor.
55   scale.tare(); //Assuming there is no weight on the scale at start up, ...
         reset the scale to 0.
56 }
57
58 //Loop, Runs forever.
59 void loop() {
60
61   //Print current load cell scale values in kg.
62   Serial.print("Reading: ");
63   currentLoad = scale.get_units(); //Acquire current applied load.
64   Serial.print(currentLoad, 1); //Print current load.
65   Serial.print(" kg ");
66
67
68   //Calculate current weight that is applied to the scale
69   //and remaps into the currect scale.
70   //The value is the sent to the ESC.
71   if (currentLoad ≥ MinSpeedWeight && currentLoad ≤ ...
         MaxSpeedWeight+errorIntervall){
72     esc.writeMicroseconds(map(abs(currentLoad), MinSpeedWeight , ...
           MaxSpeedWeight, 1000, 2000));
73     Serial.print(map(abs(currentLoad), MinSpeedWeight , MaxSpeedWeight, 0, ...
           100), 1);
74
75   }
76   //The load is too high, a warning sound is emitted.
77   else if (currentLoad ≥ MaxSpeedWeight + errorIntervall){
78     esc.writeMicroseconds(1500); //Speed forced to 50%
79     Serial.print("WARNING! 50");
80       //Play warning sound
81       for (int i = 0; i ≤ 3; i++) {
82         digitalWrite(speakerPin, HIGH);
83         delay(10);
84         digitalWrite(speakerPin, LOW);
85         delay(50);
86       }
87     }
88   //Load is below required, Don't move motor.
89   else{
90     esc.writeMicroseconds(1000);
91     Serial.print("0");
92   }
93   Serial.print(" procent");
94   Serial.println();
95 }
```

Appendix C

Simulation Code

C.1 MATLAB Code

```
%Electric Self Propelled Shoe
%Bachelors Thesis MF133X
%Authors: Viktor Karefjard & David Stridfeldt
%Date: 2021  0 2
%Description: This code calculates an approximation of
%different aspect regarding the drivetrain.

clear; clc; close all;

%% Battery voltage

n = 6; %number of LiPo cells [1]
U = 3.7*n; %Battery voltage [V]

%% Gearing and speed calculations

KV = 270; % [rpm/V]
%Gearing is not used in the prototypes current configuration,
%but is still in the code as different configurations was analysed.
r_gear_1 = 0.03;%radius [m]
r_gear_2 = 0.03;%radius [m]
r_wheel = 0.051;%radius [m]

n_motor = KV*U; %Rotational speed motor [rpm]
n_wheel = n_motor *r_gear_1/r_gear_2; %Rotational speed driven ...
    wheel [rpm]

v_max = n_wheel*2*pi*r_wheel/60*3.6 %Non-load top speed [m/s]

%% Energy calculations
%Global constants
g = 9.82; %gravitational acceleration [m/s^2]
m = 85; %total mass [kg]
```

```
33 v = 15/3.6; %velocity [m/s]
34 theta = 1*pi/180; %Slope angle [rad]
35
36 %Air resisance
37 C = 1.2; %aerodynamic resistance koeficcient
38 rho = 1.225; %Air density [kg/m^3]
39 A = 0.75; %projected area in the direction of travel [m^2]
40
41 F_air = 1/2*C*rho*A*v^2; %Total air resitance [N]
42
43 %Gravitational resistance
44 F_g = m*g*sin(theta); %[N]
45
46 %Bearing and Rolling resistance
47 my_f = 0.0015; %friction coefficient [1]
48 F_load = m*g; %load on bearing [N]
49 Crr = 0.003; %rolling resistance coefficient [1]
50
51 F_bea = my_f * F_load; %Bearing resistance [N]
52 F_roll = Crr*F_load; %Rolling resistance [N]
53
54 %Calculated effect in and out of motor
55 W_out = v*(F_bea + F_g + F_air + F_roll) %Power from motor [W]
56 W_in = W_out/0.7 %Power from battery [W]
57 M = r_wheel*(F_bea + F_g + F_air + F_roll) %Motor torque (no ...
       gearing)[Nm]
58
59 %Calculated battery capacity
60 d = 3000; %Distance traveled [m]
61 E = W_in * d/v
62 Q = E/60/60/U*1000 %Battery capacity [mAh]
63 Q_batt = Q / 0.7
64 C = W_in/U/Q_batt*1000 %Discharge rate [1/h]
65
66 MaxI = W_in/U %Maximum continous current [A]
```

C.2 ACUMEN Code

```
// Electric Self Propelled Shoe
// Bachelors Thesis MF133X
// Authors: David Stridfeldt, Viktor Karefjard
// Date: 2021 03
// Description: ACUMEN Simulation of electrically propelled shoes
// using differential equations.

// Main simulation model
model Main(simulator) =

//Initial conditions being set for the main simulation, this includes
//creating two shoe models, which in turn include two leg models.
initially // Initial conditions
 shoe1 = create Shoe((0,0,0),pi/8), //Creates shoe with leg angle
 shoe2 = create Shoe((0,0,0),-pi/8), //Creates another shoe with leg angle
 x = 0, x' = 1, x'' = 0, //Position, speed, acceleration
 F_gx = 0, F_gy = 0, F_lag = 0, F_luft = 0, F_rull = 0, // Initiall forces
 m = 80, //Mass
 g = 9.82, //Gravitational acceleration
 theta = 0*5*pi/180, //Ground angle
 my_lag = 0.0015, //Coeficient of frition in bearings
 C = 1.2, //Drag coefficient
 rho = 1.225, //Air denisty
 A = 0.75, //Projectet frontal area of person with shoes
 W_motor = 250 //Motor power output


//Defines the main simulation loop, and each variables calculated effect on
//the acceleration, speed and postion.
always
  F_luft = 1/2*C*rho*A*(x')^2, //Calculated air resistance force
  x'' = 1/m*(-F_rull - F_lag - F_gx - F_luft + W_motor/x'), //Calculates acceleration
  shoe1.pos = (x,0,0), //Sets the position of shoe 1
  shoe2.pos = (x+10,0,0) //Sets the position of shoe 2


//Creates model of the shoes
//Inpus parameters: position of shoe and rotation of leg
model Shoe(pos,rot) =
initially
 _3D = (), _Plot=(),
 leg1 = create Leg(pos,(0,rot,0)) //Creates a leg for this shoe

always //Defines visuals, which changes postion with x
 _3D = (Box center = pos + (0,0,0)
             color = blue
             width = 1
             height = 0.4
             length = 2.6,

        Box center = pos + (-0.25,0,0.25)
             color = blue
             width = 0.8
             height = 0.1
             length = 2,

        Box center = pos + (-0.75,0,0.4)
            color = blue
            width = 0.8
```

```
            height = 0.2
            length = 1

        ),
 leg1.pos = pos //Updates position of leg

//Creates model of the legs
//Inpus parameters: position and rotation of leg
model Leg(pos,rotation) =
initially
 _3D = (), _Plot=()

always //Defines visuals, which changes postion with x
 _3D = (Box
            color = yellow
            width = 0.6
            height = 10
            length = 0.8
            rotation = rotation
            //Positions leg corectly with regards to the shoes
            center = pos + (sin(rotation(1))*10/2,0,0) + (-0.75,0,5.4)
            )
```

TRITA ITM-EX 2021:27